



An E115A Missense Variant in *CERS2* Is Associated With Increased Sleeping Energy Expenditure and Hepatic Insulin Resistance in American Indians

Sascha Heinitz,^{1,2,3} Michael Traurig,¹ Jonathan Krakoff,¹ Philipp Rabe,⁴ Claudia Stäubert,⁴ Sayuko Kobes,¹ Robert L. Hanson,¹ Michael Stumvoll,^{2,3} Matthias Blüher,^{2,3} Clifton Bogardus,¹ Leslie Baier,¹ and Paolo Piaggi^{1,5}

Diabetes 2024;73:1361–1371 | <https://doi.org/10.2337/db23-0690>

Genetic determinants of interindividual differences in energy expenditure (EE) are largely unknown. Sphingolipids, such as ceramides, have been implicated in the regulation of human EE via mitochondrial uncoupling. In this study, we investigated whether genetic variants within enzymes involved in sphingolipid synthesis and degradation affect EE and insulin-related traits in a cohort of American Indians informative for 24-h EE and glucose disposal rates during a hyperinsulinemic-euglycemic clamp. Association analysis of 10,084 genetic variants within 28 genes involved in sphingolipid pathways identified a missense variant (rs267738, A>C, E115A) in exon 4 of *CERS2* that was associated with higher sleeping EE (116 kcal/day) and increased rates of endogenous glucose production during basal (5%) and insulin-stimulated (43%) conditions, both indicators of hepatic insulin resistance. The rs267738 variant did not affect ceramide synthesis in HepG2 cells but resulted in a 30% decrease in basal mitochondrial respiration. In conclusion, we provide evidence that the *CERS2* rs267738 missense variant may influence hepatic glucose production and postabsorptive sleeping metabolic rate.

Obesity manifests because of a persistent energy imbalance caused by caloric intake exceeding energy expenditure (EE). We have previously shown that 24-h EE is an inherited trait (~50% heritability) in American Indians and that lower EE contributes to long-term gains in body

ARTICLE HIGHLIGHTS

- The genetic determinants of interindividual differences in energy expenditure (EE) are not well established. Sphingolipids have been proposed to influence EE by altering mitochondrial function.
- Association analysis of genetic variants in genes involved in sphingolipid pathways identified a missense variant (rs267738, A>C, E115A) in *CERS2* associated with higher sleeping EE assessed by whole-room indirect calorimetry.
- The rs267738 variant was associated with increased glucose production under basal and insulin-stimulated conditions and with decreased basal mitochondrial respiration.
- The rs267738 missense variant may affect the expression of key gluconeogenic genes *G6PC1* and *PCK1*.

weight and fat mass in this group (1–4). We have also shown that EE and hepatic glucose output are linked in this population. For example, components of 24-h EE, i.e., resting metabolic rate and sleeping EE, along with endogenous glucose production (a marker of hepatic insulin resistance [HIR]), are higher in individuals with impaired glucose tolerance and type 2 diabetes (5,6), and higher resting metabolic

¹Phoenix Epidemiology and Clinical Research Branch, National Institute of Diabetes and Digestive and Kidney Diseases, Phoenix, AZ

²Department of Internal Medicine, Clinic for Endocrinology, Nephrology and Rheumatology, University of Leipzig, Leipzig, Germany

³Helmholtz Institute for Metabolic, Obesity and Vascular Research (HI-MAG) of the Helmholtz Zentrum München at the University of Leipzig, Philipp-Rosenthal-Strasse 27, Leipzig, Germany

⁴Faculty of Medicine, Rudolf Schönheimer Institute of Biochemistry, Leipzig University, Leipzig, Germany

⁵Department of Information Engineering, University of Pisa, Pisa, Italy

Corresponding author: Paolo Piaggi, paolo.piaggi@nih.gov

Received 29 August 2023 and accepted 20 May 2024

This article contains supplementary material online at <https://doi.org/10.2337/figshare.25864279>.

Clinical trials reg. no. NCT00340132, clinicaltrials.gov

© 2024 by the American Diabetes Association. Readers may use this article as long as the work is properly cited, the use is educational and not for profit, and the work is not altered. More information is available at <https://www.diabetesjournals.org/journals/pages/license>.

rate in the postabsorptive state correlates with higher rates of hepatic glucose production (6,7). Identifying genetic variants influencing both EE and glucose metabolism will provide insight into metabolic pathways underlying the pathogenesis of obesity and related metabolic disorders, such as insulin resistance.

Sphingolipids are molecules involved in cellular signaling and bioenergetics (8,9). Prolonged lipid excess can lead to the accumulation of ceramides, a type of sphingolipid that can alter cellular function and influence the development of type 2 diabetes, nonalcohol steatohepatitis, and cardiovascular disease (10–12). For instance, in obesity, cellular accumulation of ceramides leads to inhibition of mitochondrial respiration (11,13–15). Consistent with the detrimental effects of excess ceramides on organ metabolic function, we have shown in previous studies involving individuals with obesity that elevated skeletal muscle sphingolipid levels are associated with reduced sleeping EE, the largest component of 24-h EE in sedentary conditions, and predict greater future weight gain (16,17). This inverse correlation explained up to 16% of the interindividual variance in sleeping EE in these individuals (16,17). These and other studies point to sphingolipids/ceramides as relevant players in the control of energy balance, and their measurement in plasma is increasingly used as a diagnostic tool (18). Therefore, genetic variation in enzymes involved in sphingolipid synthesis and degradation may contribute to the development of obesity and obesity-related disorders via effects on energy metabolism. The aim of this study was to investigate whether genetic variants in sphingolipid-related genes influence whole-body EE and insulin resistance in American Indians.

RESEARCH DESIGN AND METHODS

Additional methods are provided in the Supplementary Methods.

Study Participants

Data for this study were obtained from 7,701 American Indians (19) who participated in a genome-wide association study (20). Of these participants, a subset ($n = 557$) underwent clinical measurements of glucose disposal rates during hyperinsulinemic-euglycemic clamps (HECs). Of these individuals, 419 also had measurements of 24-h EE by whole-room indirect calorimetry. Both measurements were performed at our inpatient clinical research unit at the Phoenix Epidemiology and Clinical Research Branch of the National Institute of Diabetes and Digestive and Kidney Diseases in Phoenix, Arizona (ClinicalTrials.gov identifier NCT00340132). The study protocol was approved by the National Institute of Diabetes and Digestive and Kidney Diseases institutional review board, and all participants provided written informed consent.

Clinical Characteristics for the Inpatient Subset

On admission to the clinical research unit, all participants were free from disease (except obesity) based on their

medical history, physical examination, and standard laboratory tests and received a standardized, unit-specific weight-maintaining diet (WMD) (50% carbohydrate, 30% fat, 20% protein) based on weight and sex (21). Diets were adjusted throughout the stay to ensure weight maintenance within 1% of the weight measured on the day of admission. Body fat mass (FM), fat-free mass (FFM), and percent body fat were estimated by underwater weighing until 1993 or by X-ray absorptiometry (DPX-1; Lunar Radiation Corp., Madison, WI). Values from different techniques were made comparable using a conversion equation (22). Glucose tolerance was assessed by a 75-g oral glucose tolerance test, and only individuals without diabetes based on the American Diabetes Association diagnostic criteria underwent whole-room indirect calorimetry and HEC.

Whole-Room Indirect Calorimetry

After 3 days of a WMD followed by an overnight fast, EE was continuously measured for 23.25 h starting at 0700 h inside a whole-room indirect calorimeter as previously described (23). During their stay in the calorimeter, participants were given a WMD diet consisting of four balanced meals provided at 0800, 1100, 1600, and 1900 h through an airlock to measure 24-h energy balance (24). Twenty-four-hour respiratory quotient (CO_2 production / O_2 consumption) was calculated for each 15-min interval during the 23.25 h, averaged, and extrapolated to 24 h. Based on the 24-h respiratory quotient and O_2 consumption rate (OCR), 24-h EE was calculated using the Lusk equation (25). Sleeping EE was calculated as the average EE during all 15-min intervals between 0100 and 0500 h when measurements of spontaneous physical activity by radar sensors were $<1.5\%$ (26).

HECs

HECs were performed after a 12-h overnight fast (27,28). An antecubital venous catheter was used to administer [$3\text{-}^3\text{H}$]glucose, glucose, and insulin during basal and insulin infusion phases. Blood draws were done using a retrograde catheter placed in the contralateral hand warmed by a heated (70°C) blanket. During the basal phase, [$3\text{-}^3\text{H}$]glucose was administered as a bolus ($30\ \mu\text{Ci}$) followed by a continuous infusion of [$3\text{-}^3\text{H}$]glucose at $0.30\ \mu\text{Ci}/\text{min}$. After 2 h of [$3\text{-}^3\text{H}$]glucose infusion, four plasma samples were collected during 30-min intervals for assessment of [$3\text{-}^3\text{H}$]glucose-specific activity and calculation of the endogenous glucose production rate during the basal phase (27,29). This was followed by a primed continuous infusion of insulin at $40\ \text{mU}/\text{m}^2$ body surface area per minute (Novolin; Novo Nordisk, Bagsværd, Denmark). Five minutes after insulin infusion, a variable 20% glucose infusion was started and continuously adjusted over the next 60 min to achieve a stable (coefficient of variation $<5\%$) plasma concentration of $100\ \text{mg}/\text{dL}$. The rate of glucose infusion was then measured while maintaining a stable plasma glucose concentration for the next 40 min. The rate of total

insulin-stimulated glucose disposal, adjusted for steady-state plasma glucose and insulin concentrations and then normalized for body size, was derived from the rate of exogenous glucose infusion and the rate of endogenous glucose production calculated using the Steele nonsteady-state equation (29) during this 40-min period.

Association Analyses

Genotypes were derived from a previous genome-wide association study using a custom Axiom array (Affymetrix, Santa Clara, CA) designed to capture common variation in this population (20). Genotypes were imputed from 515,723 array variants with a reference panel based on whole-genome sequences from 266 members of the population using IMPUTE2 (30) as previously described (31). Only variants with an average allele dosage between 0.01 and 1.99 copies were included in the analyses. To identify genetic variants in sphingolipid metabolism genes that may be associated with EE, imputed variants ($n = 10,084$) located 50 kb upstream and downstream of 28 genes involved in sphingolipid metabolism (32) (Supplementary Table 1) were selected for association analyses using the 419 participants informative for EE-related traits. Association analyses were performed using linear mixed-effects models taking into account relationships between individuals estimated from genomic similarity among pairs of individuals across all markers (33) and adjusting for genetic admixture, age, sex, and body composition (34,35). To confirm the imputed genotypes for rs267738, the variant was genotyped in the DNA samples using a TaqMan genotyping assay (Thermo Fisher Scientific, Waltham, MA). Statistical analyses were performed using SAS 9.4 (SAS Institute, Cary, NC) and GraphPad Prism 9.1 (GraphPad Software, San Diego, CA) software.

Data and Resource Availability

The data sets analyzed in the current study are not publicly available but are available from the corresponding author upon reasonable request and institutional review board approval.

RESULTS

Association Analyses

To determine whether variants located in or near sphingolipid metabolism genes contribute to differences in whole-body EE, a total of 10,084 imputed polymorphisms located within and surrounding (50 kb upstream and downstream) 28 genes involved in sphingolipid synthesis and degradation (Supplementary Table 1) were analyzed for associations with different daily EE measurements, e.g., 24-h and sleeping EE. Clinical characteristics for the participants informative for EE are shown in Table 1. The component of daily EE showing the strongest associations with the imputed variants was sleeping EE, and the results for all 10,084 imputed variants are reported in Supplementary Table 2. The top 10 variants significantly associated with sleeping EE are located within or near

CERS2, *SPTLC3*, *ASAH2*, and *SGMS1* (Table 2). The strongest association was with an E115A (rs267738, A>C) amino acid change in *CERS2*, where individuals carrying the C allele had, on average, higher sleeping EE ($\beta = 116$ kcal/day, $P = 3.2 \times 10^{-5}$, C-allele frequency = 0.05) (Table 2 and Fig. 1A), despite similar daytime EE ($P = 0.27$). This association was independent of FFM (Fig. 1B). There were no significant differences in measures of obesity (BMI, FM, FFM, percent body fat) between individuals heterozygous for AC and homozygous for AA ($P > 0.05$, data not shown). Individuals heterozygous for the C allele also had modestly higher endogenous glucose production rates during basal conditions ($\beta = 0.09$ mg/kg FFM/min, $P = 0.03$) (Fig. 1C) and insulin infusion ($\beta = 0.13$ mg/kg FFM/min, $P = 0.05$) (Fig. 1C), despite no differences in total insulin-stimulated glucose disposal rates ($P = 0.79$) or absolute suppression of the endogenous glucose production rate ($P = 0.82$).

Ceramide Measurements

CERS2 is mainly involved in the synthesis of very-long chain fatty acyl (VLCFA) ceramides using C20–C26 fatty acids as substrates. Therefore, we assessed the impact of *CERS2* knockout and *CERS2* E115A on ceramide synthesis using HepG2-*CERS2*^{-/-} and HepG2-*CERS2*^{-/-} cells transfected with *CERS2* expression plasmids (p*CERS2*) containing either the rs267738 A allele (p*CERS2*^A) or C allele (p*CERS2*^C) without and with palmitate supplementation. Forty-eight hours after transfection, HepG2-*CERS2*^{+/+}, HepG2-*CERS2*^{-/-}, HepG2-p*CERS2*^A, and HepG2-p*CERS2*^C cells were collected for ceramide measurements. As expected, levels for several VLCFA Cer d18:1 subspecies were decreased in the HepG2-*CERS2*^{-/-} cells compared with the HepG2-*CERS2*^{+/+} cells (Fig. 2A); however, there were no significant differences in VLCFA ceramide levels between the HepG2-p*CERS2*^A and HepG2-p*CERS2*^C cells (Fig. 2B). There were no differences in long chain fatty acyl (LCFA) Cer d18:1/16:0 and Cer d18:1/18:0 levels (data not shown). As with the HepG2 cells without palmitate treatment, levels for various VLCFA Cer d18:1 ceramides were decreased in HepG2-*CERS2*^{-/-} cells, and there were no differences in ceramide levels between HepG2-p*CERS2*^A and HepG2-p*CERS2*^C when the medium was supplemented with palmitate (data not shown). For the palmitate-treated HepG2-*CERS2*^{-/-} cells, there was a modest increase (not statistically significant) in LCFA Cer d18:1/16:0 and decreases in Cer d18:0/16:0 and Cer d18:2/16:0 compared with HepG2-*CERS2*^{+/+} cells (Fig. 2C). The *CERS2* knockout also resulted in significant decreases for various VLCFA Cer d18:2 subspecies and hexacylceramides. In line with previous studies, we also observed decreases in several VLCFA sphingomyelins for the HepG2-*CERS2*^{-/-} cells (Supplementary Fig. 1A–C).

Differential Gene Expression Analysis

Since the E115A variant is in the N-terminal homeodomain of *CERS2*, a domain thought to be involved in DNA binding and transcription regulation (Supplementary Fig. 2),

Table 1—Clinical characteristics for the study participants informative for 24-h EE measurements

	All	Males	Females	rs267738	
				A/A	A/C
<i>n</i>	419	254	165	390	29
Age (years)	27.8 ± 6.4	27.8 ± 6.6	27.8 ± 6.2	27.8 ± 6.4	26.2 ± 5.9
Body weight (kg)	95.3 ± 22.3	98.6 ± 22.7	90.2 ± 20.7	95.6 ± 22.1	97.1 ± 24.5
BMI (kg/m ²)	34.2 ± 7.5	33.4 ± 7.3	35.3 ± 7.7	34.4 ± 7.4	33.6 ± 8.8
Body fat (%)	32.6 ± 8.2	28.7 ± 6.9	38.8 ± 6.0	33.0 ± 8.0	30.4 ± 9.2
FM (kg)	32.0 ± 13.0	29.5 ± 12.9	35.8 ± 12.2	32.4 ± 12.8	31.0 ± 15.3
FFM (kg)	63.3 ± 12.6	69.0 ± 10.9	54.4 ± 9.5	63.2 ± 12.5	66.1 ± 12.4
Fasting plasma glucose concentration (mg/dL)	88.8 ± 10.0	87.3 ± 9.9	91.2 ± 9.7	88.9 ± 10	87.9 ± 9.8
2-h Plasma glucose concentration (mg/dL)	123.0 ± 30.5	115.8 ± 30.0	134.0 ± 28.0	123.2 ± 30.8	116.7 ± 27.6
24-h Energy intake (kcal/day)	2,269 ± 336	2,415 ± 286	2,043 ± 279	2,267 ± 338	2,351 ± 346
24-h EE (kcal/day)	2,354 ± 396	2,531 ± 347	2,083 ± 303	2,350 ± 391	2,475 ± 421
24-h Energy balance (kcal/day)	−83 ± 183	−108 ± 180	−43 ± 182	−83 ± 182	−124 ± 205
Sleeping EE (kcal/day)	1,672 ± 284	1,776 ± 271	1,513 ± 223	1,661 ± 274	1,830 ± 349
Spontaneous physical activity (%)	7.5 ± 2.5	7.7 ± 2.5	7.1 ± 2.5	7.5 ± 2.5	7.7 ± 2.6

Data are mean ± SD.

whole-genome RNA sequencing was performed for HepG2-*CERS2*^{+/+}, HepG2-*CERS2*^{-/-}, and two separate HepG2-*CERS2*^{-/-} clones both transfected with p*CERS2*^A and p*CERS2*^C to determine whether *CERS2* influences gene expression. When comparing gene expression levels between the HepG2-*CERS2*^{+/+} and HepG2-*CERS2*^{-/-} cells, there were 1,706 genes downregulated (\log_2 fold change ≤ -1.0) and 2,129 genes upregulated (\log_2 fold change ≥ 1.0) with $P \leq 0.009$ (false discovery rate [FDR] $P < 0.04$) in the HepG2-*CERS2*^{-/-} cells. Kyoto Encyclopedia of Genes and Genomes pathway analysis was performed for the combined list of up- and downregulated genes. One of the significantly enriched pathways was oxidative phosphorylation, which is

associated with mitochondrial function (FDR $P = 1.8 \times 10^{-18}$). There were also several differentially expressed genes in both the insulin signaling ($n = 36$) and glycolysis/gluconeogenesis ($n = 19$) pathways. However, these two pathways did not reach statistical significance (Supplementary Table 3). The HepG2-*CERS2*^{-/-} also affected the expression of various genes involved in mitochondrial dynamics and biogenesis (Supplementary Table 4). To examine the effects of HepG2-*CERS2*^{-/-} on mitochondrial content, we determined mtDNA copy number by quantitative PCR (qPCR) for two mtDNA genes: *ND1*, which is encoded on the heavy strand, and *ND6*, which is encoded on the light strand. There were no significant differences in mtDNA copy

Table 2—Top 10 imputed variants associated with sleeping EE

Variant	Gene	Allele 1	Allele 2	Dosage*	Location	Effect (kcal/day)	SE (kcal/day)	<i>P</i>
rs267738	<i>CERS2</i>	A	C	1.93	Exonic (missense)	−115.8	27.9	3.2×10^{-5}
rs267733	<i>ANXA9</i>	A	G	1.94	Exonic (missense)	−107.7	29.0	2.1×10^{-4}
rs607518	<i>ANXA9</i>	G	A	1.93	Promoter	−101.2	28.3	3.6×10^{-4}
rs198325	<i>CERS2, SETDB1</i>	C	T	1.93	Intergenic	−101.3	28.4	3.6×10^{-4}
rs33925685	<i>SPTLC3</i>	A	—	1.66	Intronic	49.2	14.2	5.2×10^{-4}
rs267734	<i>CERS2, ANXA9</i>	T	C	1.94	Intergenic	−102.6	29.6	5.3×10^{-4}
rs2842131	<i>ASAH2, SGMS1</i>	C	T	0.77	Intergenic	−35.3	10.3	6.1×10^{-4}
rs6105029	<i>SPTLC3</i>	C	T	1.65	Intronic	46.3	13.5	6.1×10^{-4}
rs6109675	<i>SPTLC3</i>	G	A	1.65	Intronic	46.3	13.5	6.1×10^{-4}
rs6514361	<i>SPTLC3</i>	T	C	1.65	Intronic	46.3	13.5	6.1×10^{-4}

Sleeping EE was adjusted for age, sex, FM, FFM, and genetic admixture. Effects (β -coefficients) refer to allele 1. *P* values were controlled for inflation by the genomic control method. *All imputed variants tested had a mean dosage for allele 1 between 0.01 and 1.99 copies as calculated in 419 samples informative for sleeping EE and imputed genotypes (Table 1).

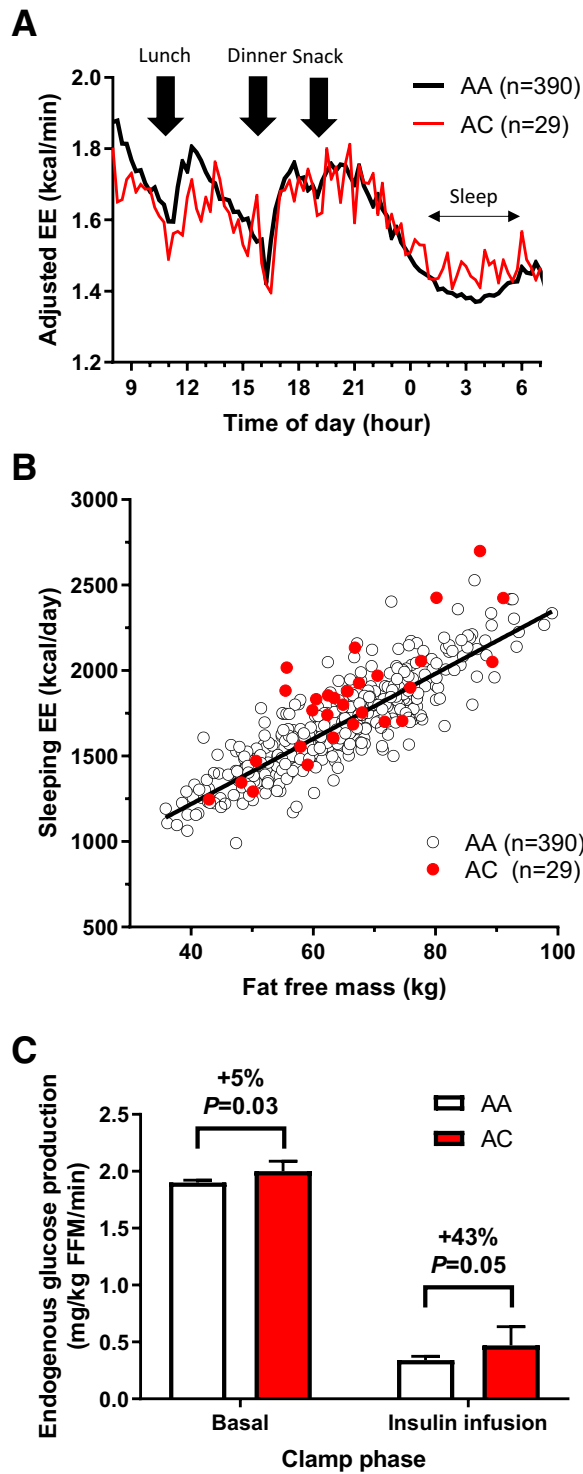


Figure 1—Differences in 24-h EE and endogenous glucose production based on rs267738 genotypes. **A:** Time course of EE over 24 h inside the whole-room indirect calorimeter during isocaloric conditions for individuals homozygous (AA) or heterozygous (AC) for rs267738. EE was adjusted for age, sex, FM, FFM, spontaneous physical activity, and genetic admixture using linear mixed models. **B:** Correlation between FFM and sleeping EE measured overnight inside the whole-room indirect calorimeter in individuals homozygous (AA) or heterozygous (AC) for rs267738. **C:** Glucose disposal rates assessed during the basal and insulin infusion phases of the HEC. Rates were normalized to FFM as determined by underwater weighing or by X-ray absorptiometry.

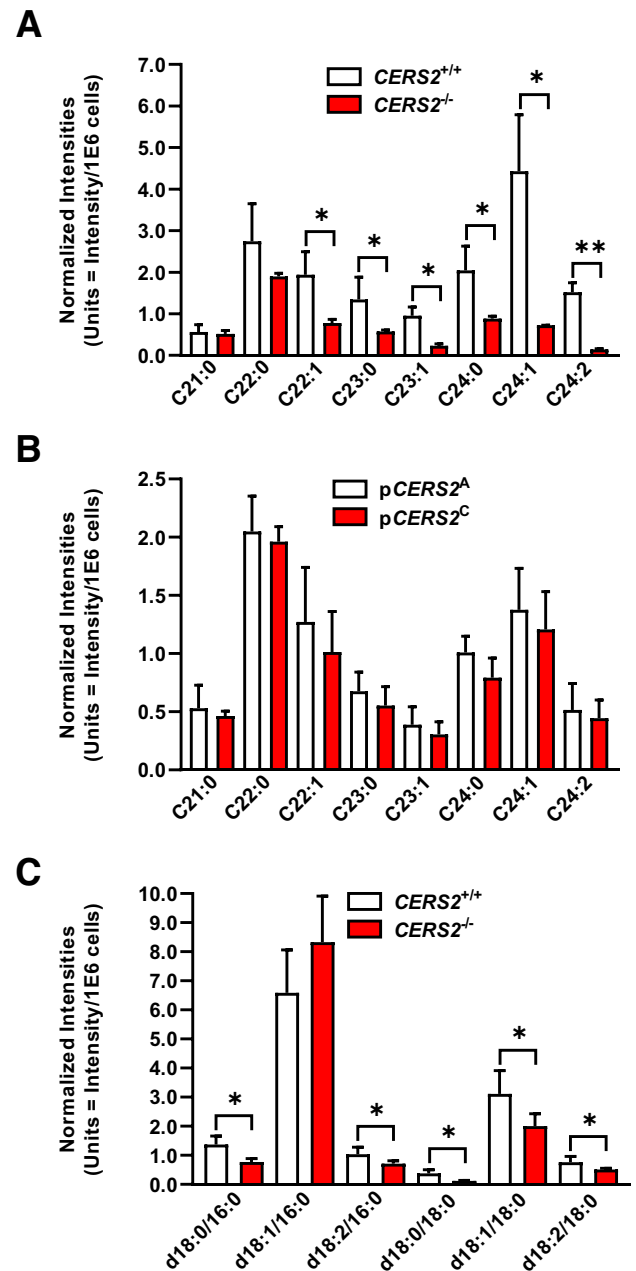


Figure 2—Liquid chromatography-mass spectrometry measurements of VLCFA and LCFA ceramides. **A:** Normalized intensities for VLCFA Cer d18:1 ceramides in HepG2-*CERS2*^{+/+} and HepG2-*CERS2*^{-/-} cells. **B:** Normalized intensities for VLCFA Cer d18:1 ceramides in HepG2-*CERS2*^{-/-} cells carrying either p*CERS2*^A or p*CERS2*^C. **C:** Normalized intensities for LCFA ceramides in HepG2-*CERS2*^{+/+} and HepG2-*CERS2*^{-/-} cells. Data are mean ± SD (n = 3). *P ≤ 0.05, **P < 0.01.

number between HepG2-*CERS2*^{+/+} and HepG2-*CERS2*^{-/-} cells (Supplementary Fig. 3A). The similar mtDNA copy numbers may be a result of increased *TFAM* gene expression for the HepG2-*CERS2*^{-/-} cells, offsetting the decrease in *SIRT1* and *PPARGC1A* expression (Supplementary Table 4).

When comparing gene expression levels between the HepG2-p*CERS2*^A and HepG2-p*CERS2*^C cells, there were 38 genes upregulated in the HepG2-p*CERS2*^C cells with

\log_2 fold change ≥ 1.0 and $P \leq 0.009$; however, only 16 remained significant after FDR correction. Of these 16 differentially expressed genes, 12 are encoded on the mtDNA (Supplementary Table 5). To determine whether the upregulation of mitochondrial genes for the HepG2-pCERS2^C cells corresponded to an increase in electron transport chain activity, we examined complex I (NADH dehydrogenase) enzyme activity. NADH dehydrogenase activity was analyzed using equal amounts of whole-cell protein extracts prepared from HepG2-pCERS2^A and HepG2-pCERS2^C cells, and enzyme activity was expressed as change in absorbance per minute. NADH dehydrogenase activity for the HepG2-pCERS2^C cells was higher than for the HepG2-pCERS2^A cells ($P = 0.008$) (Supplementary Fig. 4). The increase in mitochondrial gene expression for HepG2-pCERS2^C cells does not appear to be due to an increase in mtDNA copy number (Supplementary Fig. 3B), which coincides with the RNA sequencing data showing that there is no difference in expression for mitochondrial biogenesis genes between the CERS2^A and CERS2^C alleles (data not shown). Two genes with slightly lower expression levels for the HepG2-pCERS2^C cells, *PGM1* (top downregulated gene) (Supplementary Table 5) and *GAPDH* (not statistically significant, data not shown), were selected for reverse transcription-quantitative polymerase chain reaction (RT-qPCR) verification because both genes are important for glycolytic activity. The RT-qPCR results confirm that both genes are downregulated in the HepG2-pCERS2^C cells (Fig. 3). We scanned the 5' regions of *PGM1* and *GAPDH* using the JASPAR

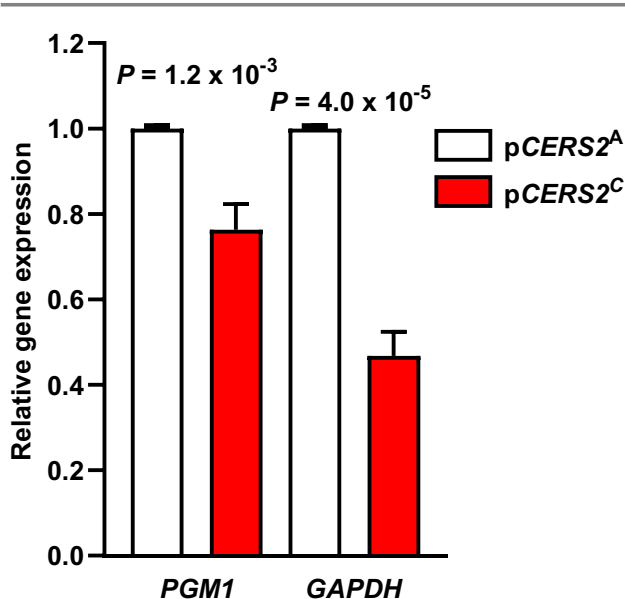


Figure 3—RT-qPCR verification for *PGM1* and *GAPDH*. Each sample was run in triplicate, and relative gene expression levels were determined using the $\Delta\Delta C_t$ method. *PGM1* and *GAPDH* gene expression levels were normalized first to *ABL1* and then to *CERS2* expression levels for each sample to normalize data across samples and to account for transfection efficiency. Data are mean \pm SD ($n = 3$).

database and identified several putative Schlank/lag1 (CerS) binding sites (Supplementary Fig. 5).

Seahorse Analyses

It has been shown that *Cers2* deficiency in mice can lead to hepatic steatosis and insulin resistance, presumably due to ceramide-induced impairment of the mitochondrial respiratory chain leading to incomplete lipid oxidation and accumulation of triglycerides (8). Therefore, we investigated the effects of E115A on mitochondrial respiration in HepG2-pCERS2^A and HepG2-pCERS2^C cells using the fatty acid palmitate as the main mitochondrial substrate. We found that basal mitochondrial respiration, assessed by measuring mitochondrial OCR, was 30% lower in the BSA controls (no exogenous palmitate) for the HepG2-pCERS2^C cells ($P = 0.01$) (Fig. 4A). There were no significant differences in maximal respiration, nonmitochondrial respiration, and glycolytic rates (extracellular acidification rate [ECAR]); however, there was a trend toward decreased glycolysis (Fig. 4B–D). Similarly, when palmitate-BSA was used as the substrate, HepG2-pCERS2^C cells had slightly lower basal respiration rates ($P = 0.05$) (Fig. 4E), and there were no significant differences in maximal respiration, nonmitochondrial respiration, and ECAR (Fig. 4F–H). However, when the outlier data points (solid squares) for palmitate basal respiration were excluded from the analyses, the differences were no longer statistically significant ($P > 0.05$). This is in line with the palmitate utilization data that also show no difference in OCR between the two alleles ($P > 0.05$) (Fig. 4I). Basal respiration rates (excluding palmitate outliers) and glycolysis (ECAR) were comparable between the cells treated with BSA only and palmitate-BSA for both the HepG2-pCERS2^A and HepG2-pCERS2^C cells ($P > 0.05$) (Fig. 4J and K). Simultaneous measurement of the relative utilization of mitochondrial respiration and glycolysis under basal and stressed conditions helped assess the metabolic phenotypes of HepG2-pCERS2^A and HepG2-pCERS2^C cells. The HepG2-pCERS2^C cells displayed a more quiescent, less aerobic metabolism compared with HepG2-pCERS2^A cells (Fig. 4L). The decrease in basal mitochondrial respiration for the HepG2-pCERS2^C cells was similar to the decrease that we observed for HepG2-CERS2^{-/-} cells; however, the reduced mitochondrial efficiencies may involve distinct mechanisms of impairment (Supplementary Fig. 6).

Effects of CERS2 E115A on AKT Phosphorylation and Gluconeogenic Gene Expression

To assess the effects of CERS2 E115A on hepatic insulin signaling, we examined AKT phosphorylation in HepG2-pCERS2^A and HepG2-pCERS2^C cells by Western blotting after treating the cells with 100 nmol/L insulin for 15 min. There were no differences in AKT Thr308 or AKT Ser473 phosphorylation between the two E115A alleles (data not shown). Next, we examined whether the E115A variant may alter the effect of insulin on cAMP-induced

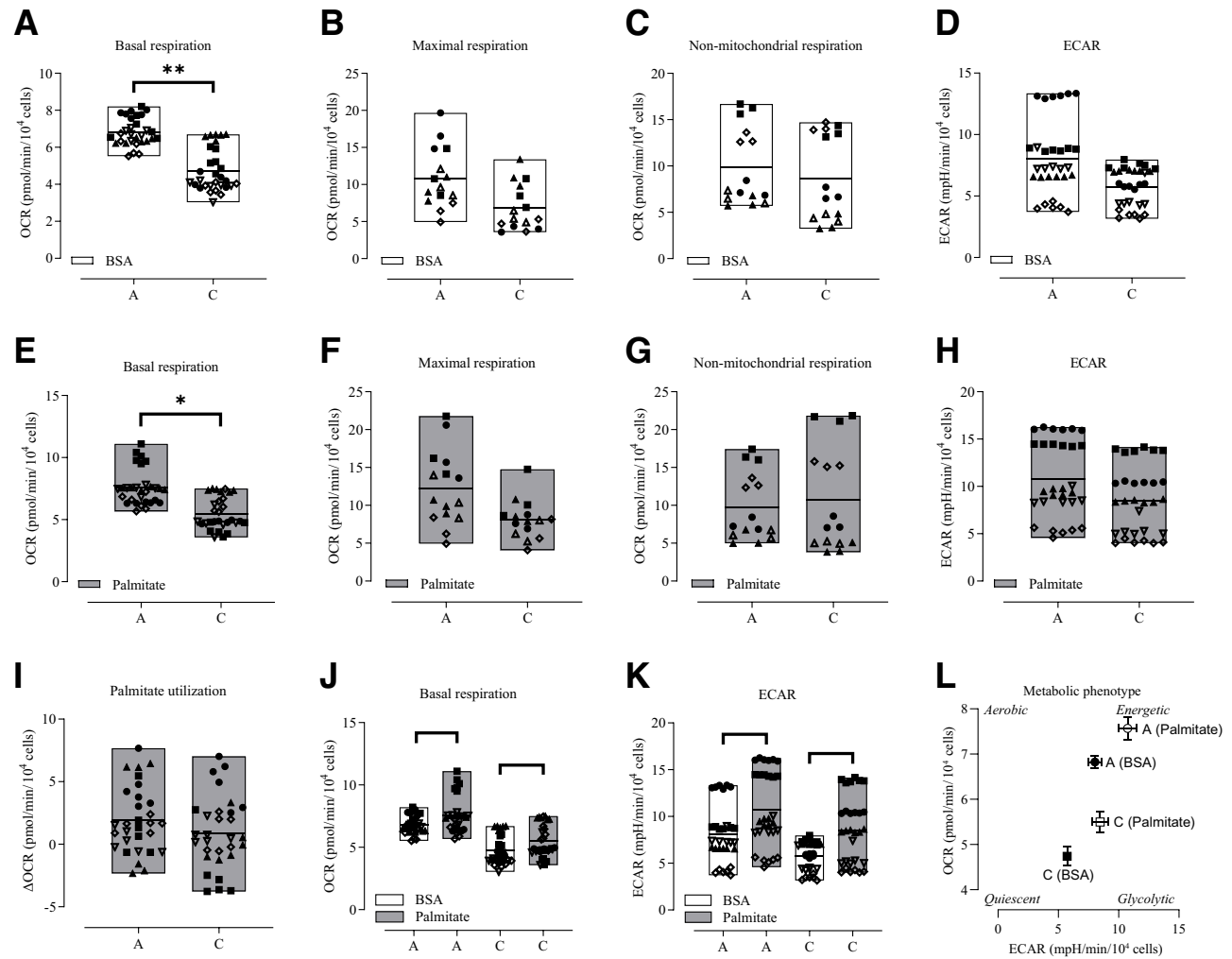


Figure 4—Mitochondrial respiratory bioenergetics in HepG2-pCERS2^A and HepG2-pCERS2^C cells. Mitochondrial respiration was studied in HepG2-CERS2^{-/-} cells transfected with either pCERS2^A (A) or pCERS2^C (C) plasmids. A–K: Individual data points are shown for each genotype group within box plots delimited by minimum and maximum values. Open box plots: BSA control, no exogenous palmitate, 2 mmol/L glucose. Shaded box plots: exogenous palmitate-BSA, 2 mmol/L glucose. A and E: Basal respiration indicates oxygen consumption at rest. B and F: Maximal respiration is the measure of maximal respiratory capacity during mitochondrial uncoupling after injection of carbonyl cyanide p-trifluoromethoxyphenylhydrazone (uncoupling reagent). C and G: Nonmitochondrial respiration indicates oxygen consumption during inhibition of electron transport chain complexes I and III after injection of rotenone and antimycin A. D and H: Glycolysis was measured indirectly by analysis of ECAR. I: Palmitate utilization after injection of the fatty acid oxidation inhibitor etomoxir. J: Comparison between BSA control and palmitate OCR during basal respiration. K: Comparison between BSA control and palmitate ECAR during basal respiration. Single experiments are indicated by the corresponding symbols ($n = 5$). Differences in OCR and ECAR between groups were tested using mixed models to account for repeated measurements from the same experiment. L: Metabolic phenotype assessed by measuring the relative utilization of mitochondrial respiration and glycolysis under basal and stressed conditions. * $P = 0.05$, ** $P = 0.01$.

gluconeogenic gene (*G6PC1*, *PCK1*) expression. After 24 h of serum starvation, HepG2-pCERS2^A and HepG2-pCERS2^C cells were treated with either insulin, dibutyryl cAMP (dbcAMP), or dbcAMP plus insulin. Gene expression levels for both *G6PC1* and *PCK1* were suppressed when the cells were treated with insulin alone, while dbcAMP significantly increased expression for both genes. The HepG2-pCERS2^C cells treated with dbcAMP had a modest increase in *G6PC1* and *PCK1* gene expression compared with the HepG2-pCERS2^A cells, suggesting that the CERS2 E115A variant may influence the expression of both genes during dbcAMP

stimulation. For the cells treated with dbcAMP plus insulin, insulin was able to suppress gene expression for both *G6PC1* and *PCK1* (Fig. 5A and B). Scanning the 5' regions of *G6PC1* and *PCK1* identified several putative Schlang/lag1 (CerS) binding sites with scores >0.90. (Supplementary Fig. 7A and B). Gene expression levels for *G6PC1* and *PCK1* were significantly decreased in HepG2-CERS2^{-/-} cells that were not subjected to serum starvation or treated with insulin and dbcAMP, suggesting that CERS2 may indeed regulate the transcription of these two genes (Supplementary Fig. 7C and D).

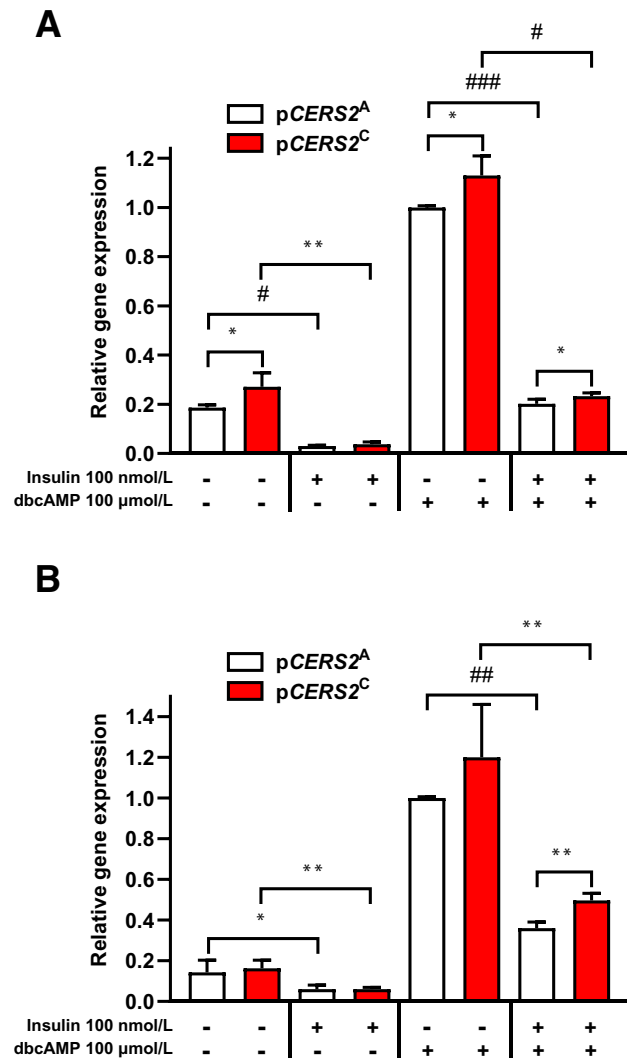


Figure 5—Analysis of gluconeogenic gene expression. *A* and *B*: RT-qPCR analysis of *G6PC1* and *PCK1* gene expression in HepG2-pCERS2^A and HepG2-pCERS2^C cells. The HepG2 cells were serum starved for 24 h and then treated with either insulin (100 nmol/L), dbcAMP (100 μmol/L), or insulin (100 nmol/L) plus dbcAMP (100 μmol/L) for 6 h. For the RT-PCR, each sample was run in triplicate, and relative gene expression levels were determined using the $\Delta\Delta C_t$ method. *G6PC1* and *PCK1* gene expression levels were normalized first to *ABL1* and then to *CERS2* expression levels for each sample to normalize data across samples and to account for transfection efficiency. Data are shown relative to HepG2-pCERS2^A treated with dbcAMP alone. Data are mean \pm SD ($n = 3$). * $P < 0.05$, ** $P < 0.01$, # $P < 1 \times 10^{-4}$, ### $P < 1 \times 10^{-5}$, #### $P < 1 \times 10^{-6}$.

DISCUSSION

In this study, we conducted an association analysis involving EE and insulin-related traits and $\sim 10,000$ imputed variants within or near several sphingolipid metabolism genes in American Indians informative for EE. The analysis identified an E115A (rs267738, A>C, minor allele frequency = 0.05) missense variant in *CERS2* that was significantly associated with sleeping EE and modestly associated with HIR and hepatic glucose output. Individuals heterozygous for the C allele had relatively higher sleeping

EE (116 kcal/day or 8% sleeping metabolic rate) compared with individuals homozygous for the A allele. Individuals carrying the C allele also had higher (43%) rates of endogenous glucose production during the insulin infusion phase of HEC along with higher (5%) rates of endogenous glucose production in the postabsorptive state during the basal phase of HEC. The association between the *CERS2* E115A variant and HIR is consistent with previous mouse studies demonstrating that *Cers2* deficiency can lead to HIR, presumably because of altered sphingolipid composition or mitochondrial dysfunction impairing insulin signaling in hepatocytes (8,36). Furthermore, a study of E115A knockin mice fed a high-fat diet showed that mice carrying the alanine residue (encoded by the C allele) were glucose intolerant, indicating a potential impairment in glucose metabolism (37). The increased rates of sleeping EE for the C allele may reflect increased hepatic gluconeogenesis using precursors provided by the Cori and glucose-alanine cycles or the breakdown of triglycerides. Hepatic gluconeogenesis occurs primarily during fasting states, such as sleep, and is an energy-demanding process (5,28,38,39), accounting for $\sim 30\%$ of resting EE (40). However, since we do not have hepatocyte (cellular) measurements of insulin action and glucose production for the same individuals with whole-body EE, we can only hypothesize that HIR-induced gluconeogenesis underlies the increase in sleeping EE in individuals carrying the rs267738 C allele.

Previous studies have shown that sphingolipid-mediated mitochondrial dysfunction may be involved in the pathogenesis of HIR and that *Cers2* deficiency in mice results in altered ceramide levels, mitochondrial dysfunction, and HIR (41,42). Therefore, we examined the effects of E115A on ceramide synthesis and mitochondrial function using HepG2 hepatocytes. We found no differences in ceramide levels between HepG2-pCERS2^A and HepG2-pCERS2^C cells. This was similar to the results seen in the *Cers2* E115A knockin mouse study where although the amino acid change was shown to result in a decrease in enzyme activity, no significant differences in liver long-chain ceramides were seen between the A and C alleles (37). Although we did not observe any effects of E115A on HepG2 ceramide content, the variant could potentially affect sphingolipid content in peripheral tissues such as fat. The excess sphingolipids in adipose tissue can then be transported to the liver, stimulating lipid deposition and interfering with liver metabolism, which may be a possible mechanism for the observed HIR. In the *Cers2* E115A knockin mouse study, an increase in C16:0 sphingolipids in subcutaneous white adipose tissue was observed in *Cers2*^{Ala/Ala} mice (37). Unfortunately, we did not have sphingolipid measurements for individuals carrying the rs267738 C allele; therefore, it was not possible to perform association analyses between the variant and serum, adipose, or skeletal muscle sphingolipid levels. We did observe an effect of the rs267738 variant on mitochondrial bioenergetics. HepG2-pCERS2^C cells

showed a 30% decrease in basal mitochondrial respiration in the absence of exogenous fatty acids (palmitate). The similarity in basal palmitate respiration and utilization rates between the two rs267738 alleles suggests that the putative defect in cellular respiration does not involve fatty acid oxidation and is in a pathway prior to oxidative phosphorylation, such as glycolysis. Future studies are warranted to fully elucidate the role of the CERS2 E115A substitution on cellular respiration, including performing glycolysis stress tests and glucose oxidation assays to further evaluate its effect on glucose utilization.

Recent studies have suggested that CERS2 may be involved in cellular processes other than ceramide synthesis. For example, inactivation of *Cers2* in mice has been shown to alter gene expression (43,44). It has also been shown that mouse *Cers2* has the ability to regulate transcription at the promoter level and that mutations in the homeodomain (nuclear localization signal 2 motif) of mouse *Cers2* lead to a loss of transcriptional regulation. In that same study, the authors showed that Schlank (*Drosophila CerS*) can adjust DNA binding and transcriptional regulation based on energy status (45). Our differential gene expression analysis also suggests that CERS2 can affect gene expression, and it revealed a downregulation of two genes related to carbohydrate metabolism, *PGM1* and *GAPDH*, in HepG2-pCERS2^C cells. *PGM1* is involved in the bidirectional conversion of glucose-1-phosphate to glucose-6-phosphate and is important for fasting glycolysis, while *GAPDH* is mainly involved in catalyzing the sixth reaction of glycolysis (46,47). In silico analyses identified several potential CERS2 binding sites in the 5' regions of both genes. We also observed an upregulation of mtDNA-encoded genes for the HepG2-pCERS2^C cells, which may be a compensatory response to lower mitochondrial respiration, possibly caused by impaired pyruvate production/reduced pyruvate metabolism during glycolysis.

How mitochondrial impairment caused by the CERS2 E115A variant may lead to HIR is currently unclear. It has been suggested that mitochondrial dysfunction caused by impaired fatty acid β -oxidation leads to an increase in hepatic lipids, and this increase in lipids may be the mechanism behind HIR. The excess lipids lead to phosphorylation of the insulin receptor substrate, which in turn inhibits insulin signaling (48,49). However, our Seahorse analysis indicated that there is no significant difference in fatty acid (palmitate) oxidation, suggesting that there may be an alternative mechanism for CERS2 E115A-induced hepatic lipid accumulation and subsequent HIR. This is supported by the observation that *Cers2*^{Ala/Ala} mice fed a high-fat diet had increased liver triglycerides compared with *Cers2* wild-type mice (37). When examining insulin's ability to suppress gluconeogenic gene expression, we detected a modest increase in *G6PC1* and *PCK1* expression for the HepG2-pCERS2^C cells when treated with dbcAMP, and repression of dbcAMP-induced gene expression by insulin appears to

be stronger for HepG2-pCERS2^A. These results may help to explain the association between rs267738 and endogenous glucose production during the HEC. Additional studies are needed to determine if the increase in gene expression occurs in vivo and leads to increased glucose production during nocturnal hepatic gluconeogenesis. A previous study demonstrated that individuals with type 2 diabetes have higher rates of nocturnal glucose production and suggested that this in part may reflect an increase in G6PC1 activity. They also suggested that PCK1 and G6PC1 inhibitors may be useful in reducing late nocturnal hyperglycemia (50).

In conclusion, the rs267738 CERS2 homeodomain E115A variant is associated with altered energy metabolism and hepatic glucose output. Future studies are needed to determine whether mitochondrial dysfunction unrelated to fatty acid β -oxidation can lead to HIR and to verify whether the E115A variant alters DNA binding, thereby affecting transcriptional regulation of genes involved in mitochondrial energy production and during nocturnal hepatic glucose production.

Acknowledgments. The authors thank all volunteers for their participation in this study and the clinical staff and laboratory technicians of the Phoenix Epidemiology and Clinical Research Branch.

Funding. This research was supported by the Intramural Research Program of the National Institutes of Health and National Institute of Diabetes and Digestive and Kidney Diseases grant DK069015-36.

Duality of Interest. No potential conflicts of interest relevant to this article were reported.

Author Contributions. S.H. designed and performed the Seahorse experiments, analyzed and interpreted the data, and wrote the manuscript. M.T. designed and performed the in vitro experiments, analyzed and interpreted the data, and wrote the manuscript. J.K., P.R., C.S., S.K., R.L.H., M.S., M.B., and B.C. reviewed the manuscript and assisted in the interpretation of the data. L.B. designed the study, assisted in the interpretation of the data, and edited and reviewed the manuscript. P.P. designed the study, analyzed and interpreted the data, and wrote the manuscript. All authors read and approved the final version of the manuscript. P.P. is the guarantor of this work and, as such, had full access to all the data in the study and takes responsibility for the integrity of the data and the accuracy of the data analysis.

References

1. Ravussin E, Lillioja S, Knowler WC, et al. Reduced rate of energy expenditure as a risk factor for body-weight gain. *N Engl J Med* 1988;318:467–472
2. Piaggi P, Thearle MS, Bogardus C, Krakoff J. Lower energy expenditure predicts long-term increases in weight and fat mass. *J Clin Endocrinol Metab* 2013;98:E703–E707
3. Piaggi P, Krakoff J, Bogardus C, Thearle MS. Lower “awake and fed thermogenesis” predicts future weight gain in subjects with abdominal adiposity. *Diabetes* 2013;62:4043–4051
4. Chan JM, Rimm EB, Colditz GA, Stampfer MJ, Willett WC. Obesity, fat distribution, and weight gain as risk factors for clinical diabetes in men. *Diabetes Care* 1994;17:961–969
5. Piaggi P, Thearle MS, Bogardus C, Krakoff J. Fasting hyperglycemia predicts lower rates of weight gain by increased energy expenditure and fat oxidation rate. *J Clin Endocrinol Metab* 2015;100:1078–1087

6. Weyer C, Bogardus C, Pratley RE. Metabolic factors contributing to increased resting metabolic rate and decreased insulin-induced thermogenesis during the development of type 2 diabetes. *Diabetes* 1999;48:1607–1614
7. Fontvieille AM, Lillioja S, Ferraro RT, Schulz LO, Rising R, Ravussin E. Twenty-four-hour energy expenditure in Pima Indians with type 2 (non-insulin-dependent) diabetes mellitus. *Diabetologia* 1992;35:753–759
8. Raichur S, Wang ST, Chan PW, et al. *Cers2* haploinsufficiency inhibits β -oxidation and confers susceptibility to diet-induced steatohepatitis and insulin resistance [published correction appears in *Cell Metab* 2014;20:919]. *Cell Metab* 2014;20:687–695
9. Park W-J, Park J-W, Merrill AH, Storch J, Pewzner-Jung Y, Futerman AH. Hepatic fatty acid uptake is regulated by the sphingolipid acyl chain length. *Biochim Biophys Acta* 2014;1841:1754–1766
10. Sokolowska E, Blachnio-Zabielska A. The role of ceramides in insulin resistance. *Front Endocrinol (Lausanne)* 2019;10:577
11. Summers SA, Chaurasia B, Holland WL. Metabolic messengers: ceramides. *Nat Metab* 2019;1:1051–1058
12. Raichur S, Brunner B, Bielohuby M, et al. The role of C16:0 ceramide in the development of obesity and type 2 diabetes: *Cers6* inhibition as a novel therapeutic approach. *Mol Metab* 2019;21:36–50
13. Kogot-Levin A, Saada A. Ceramide and the mitochondrial respiratory chain. *Biochimie* 2014;100:88–94
14. Zigdon H, Kogot-Levin A, Park J-W, et al. Ablation of ceramide synthase 2 causes chronic oxidative stress due to disruption of the mitochondrial respiratory chain. *J Biol Chem* 2013;288:4947–4956
15. Turpin SM, Nicholls HT, Willmes DM, et al. Obesity-induced *Cers6*-dependent C16:0 ceramide production promotes weight gain and glucose intolerance. *Cell Metab* 2014;20:678–686
16. Heinitz S, Basolo A, Piomelli D, Krakoff J, Piaggi P. Endocannabinoid anandamide mediates the effect of skeletal muscle sphingomyelins on human energy expenditure. *J Clin Endocrinol Metab* 2018;103:3757–3766
17. Heinitz S, Piaggi P, Vinales KL, et al. Specific skeletal muscle sphingolipid compounds in energy expenditure regulation and weight gain in Native Americans of Southwestern heritage. *Int J Obes* 2017;41:1585–1593
18. Summers SA. Could ceramides become the new cholesterol? *Cell Metab* 2018;27:276–280
19. Knowler WC, Pettitt DJ, Saad MF, et al. Obesity in the Pima Indians: its magnitude and relationship with diabetes. *Am J Clin Nutr* 1991;53(Suppl.):1543S–1551S
20. Piaggi P, Masindova I, Muller YL, et al. A genome-wide association study using a custom genotyping array identifies variants in *GPR158* associated with reduced energy expenditure in American Indians. *Diabetes* 2017;66:2284–2295
21. Pannacciulli N, Salbe AD, Ortega E, Venti CA, Bogardus C, Krakoff J. The 24-h carbohydrate oxidation rate in a human respiratory chamber predicts ad libitum food intake. *Am J Clin Nutr* 2007;86:625–632
22. Tataranni PA, Ravussin E. Use of dual-energy X-ray absorptiometry in obese individuals. *Am J Clin Nutr* 1995;62:730–734
23. Ravussin E, Lillioja S, Anderson TE, Christin L, Bogardus C. Determinants of 24-hour energy expenditure in man. Methods and results using a respiratory chamber. *J Clin Invest* 1986;78:1568–1578
24. Abbott WG, Howard BV, Christin L, et al. Short-term energy balance: relationship with protein, carbohydrate, and fat balances. *Am J Physiol* 1988;255:E332–E337
25. Lusk G. Animal calorimetry: analysis of the oxidation of mixtures of carbohydrate and fat. *J Biol Chem* 1924;59:41–42
26. Schutz Y, Ravussin E, Diethelm R, Jequier E. Spontaneous physical activity measured by radar in obese and control subject studied in a respiration chamber. *Int J Obes* 1982;6:23–28
27. Lillioja S, Mott DM, Zawadzki JK, et al. In vivo insulin action is familial characteristic in nondiabetic Pima Indians. *Diabetes* 1987;36:1329–1335
28. Bogardus C, Lillioja S, Mott D, Zawadzki J, Young A, Abbott W. Evidence for reduced thermic effect of insulin and glucose infusions in Pima Indians. *J Clin Invest* 1985;75:1264–1269
29. Steele R. Influences of glucose loading and of injected insulin on hepatic glucose output. *Ann N Y Acad Sci* 1959;82:420–430
30. Howie BN, Donnelly P, Marchini J. A flexible and accurate genotype imputation method for the next generation of genome-wide association studies. *PLoS Genet* 2009;5:e1000529
31. Bandesh K, Traurig M, Chen P, et al. Identification and characterization of the long non-coding RNA *NFIA-AS2* as a novel locus for body mass index in American Indians. *Int J Obes* 2023;47:434–442
32. Quinville BM, Deschenes NM, Ryckman AE, Walia JS. A comprehensive review: sphingolipid metabolism and implications of disruption in sphingolipid homeostasis. *Int J Mol Sci* 2021;22:5793
33. Browning BL, Browning SR. A fast, powerful method for detecting identity by descent. *Am J Hum Genet* 2011;88:173–182
34. Piaggi P, K roglu C, Nair AK, et al. Exome sequencing identifies a nonsense variant in *DAO* associated with reduced energy expenditure in American Indians. *J Clin Endocrinol Metab* 2020;105:e3989–e4000
35. Quehenberger O, Armando AM, Brown AH, et al. Lipidomics reveals a remarkable diversity of lipids in human plasma. *J Lipid Res* 2010;51:3299–3305
36. Park JW, Park WJ, Kuperman Y, Boura-Halfon S, Pewzner-Jung Y, Futerman AH. Ablation of very long acyl chain sphingolipids causes hepatic insulin resistance in mice due to altered detergent-resistant membranes. *Hepatology* 2013;57:525–532
37. Nicholson RJ, Poss AM, Maschek JA, et al. Characterizing a common *CERS2* polymorphism in a mouse model of metabolic disease and in subjects from the Utah CAD study. *J Clin Endocrinol Metab* 2021;106:e3098–e3109
38. Ravussin E, Bogardus C, Schwartz RS, et al. Thermic effect of infused glucose and insulin in man. Decreased response with increased insulin resistance in obesity and noninsulin-dependent diabetes mellitus. *J Clin Invest* 1983;72:893–902
39. Lillioja S, Mott DM, Zawadzki JK, Young AA, Abbott WG, Bogardus C. Glucose storage is a major determinant of in vivo “insulin resistance” in subjects with normal glucose tolerance. *J Clin Endocrinol Metab* 1986;62:922–927
40. Quaye E, Chacko S, Chung ST, Brychta RJ, Chen KY, Brown RJ. Energy expenditure due to gluconeogenesis in pathological conditions of insulin resistance. *Am J Physiol Endocrinol Metab* 2021;321:E795–E801
41. Turpin-Nolan SM, Br uning JC. The role of ceramides in metabolic disorders: when size and localization matters. *Nat Rev Endocrinol* 2020;16:224–233
42. Montgomery MK, Brown SH, Lim XY, et al. Regulation of glucose homeostasis and insulin action by ceramide acyl-chain length: a beneficial role for very long-chain sphingolipid species. *Biochim Biophys Acta* 2016;1861:1828–1839
43. Pewzner-Jung Y, Brenner O, Braun S, et al. A critical role for ceramide synthase 2 in liver homeostasis: II. insights into molecular changes leading to hepatopathy. *J Biol Chem* 2010;285:10911–10923
44. Bickert A, Kern P, van Uelft M, et al. Inactivation of ceramide synthase 2 catalytic activity in mice affects transcription of genes involved in lipid metabolism and cell division. *Biochim Biophys Acta Mol Cell Biol Lipids* 2018;1863:734–749
45. Sociale M, Wulf AL, Breiden B, et al. Ceramide synthase Schlank is a transcriptional regulator adapting gene expression to energy requirements. *Cell Rep* 2018;22:967–978
46. Backe PH, Laerdahl JK, Kittelsen LS, Dalhus B, M rkr d L, Bj r s M. Structural basis for substrate and product recognition in human phosphoglucomutase-1 (PGM1) isoform 2, a member of the α -D-phosphohexomutase superfamily. *Sci Rep* 2020;10:5656

47. Ramzan R, Weber P, Linne U, Vogt S. GAPDH: the missing link between glycolysis and mitochondrial oxidative phosphorylation? *Biochem Soc Trans* 2013;41:1294–1297
48. Rector RS, Morris EM, Ridenhour S, et al. Selective hepatic insulin resistance in a murine model heterozygous for a mitochondrial trifunctional protein defect. *Hepatology* 2013;57:2213–2223
49. Crescenzo R, Bianco F, Mazzoli A, Giacco A, Liverini G, Iossa S. A possible link between hepatic mitochondrial dysfunction and diet-induced insulin resistance. *Eur J Nutr* 2016;55:1–6
50. Basu A, Joshi N, Miles J, Carter RE, Rizza RA, Basu R. Paradigm shifts in nocturnal glucose control in type 2 diabetes. *J Clin Endocrinol Metab* 2018; 103:3801–3809